JOURNAL OF THE ROYAL SOCIETY Interface

Human-like external function of the foot, and fully upright gait, confirmed in the 3.66 million year old Laetoli hominin footprints by topographic statistics, experimental footprint-formation and computer simulation

Robin H. Crompton, Todd C. Pataky, Russell Savage, Kristiaan D'Août, Matthew R. Bennett, Michael H. Day, Karl Bates, Sarita Morse and William I. Sellers

J. R. Soc. Interface 2012 **9**, 707-719 first published online 20 July 2011
doi: 10.1098/rsif.2011.0258

JOURNAL OF THE ROYAL SOCIETY Interface

J. R. Soc. Interface (2012) **9**, 707–719
doi:10.1098/rsif.2011.0258
Published online 20 July 2011

Human-like external function of the foot, and fully upright gait, confirmed in the 3.66 million year old Laetoli hominin footprints by topographic statistics, experimental footprint-formation and computer simulation

Robin H. Crompton[1,*,†], Todd C. Pataky[2,†], Russell Savage[1,†], Kristiaan D'Août[3], Matthew R. Bennett[4], Michael H. Day[5], Karl Bates[1], Sarita Morse[1,4] and William I. Sellers[6,†]

[1]*Institute of Aging and Chronic Disease, University of Liverpool, Sherrington Buildings, Ashton Street, Liverpool L69 3GE, UK*
[2]*Department of Bioengineering, Shinshu University, 3-1-15 Tokida, Ueda-shi, Nagano-ken 386-8567, Japan*
[3]*Department of Biology, University of Antwerp–Campus Drie Eiken D.C.1.08, Universiteitsplein 1, 2610 Antwerpen, Belgium*
[4]*School of Applied Sciences, Bournemouth University, Talbot Campus, Fern Barrow, Poole, Dorset BH12 5BB, UK*
[5]*Department of Palaeontology, The Natural History Museum, London SW7 5BD, UK*
[6]*Faculty of Life Sciences, University of Manchester, Oxford Road, Manchester M13 9PT, UK*

It is commonly held that the major functional features of the human foot (e.g. a functional longitudinal medial arch, lateral to medial force transfer and hallucal (big-toe) push-off) appear only in the last 2 Myr, but functional interpretations of footbones and footprints of early human ancestors (hominins) prior to 2 million years ago (Mya) remain contradictory. Pixel-wise topographical statistical analysis of Laetoli footprint morphology, compared with results from experimental studies of footprint formation; foot-pressure measurements in bipedalism of humans and non-human great apes; and computer simulation techniques, indicate that most of these functional features were already present, albeit less strongly expressed than in ourselves, in the maker of the Laetoli G-1 footprint trail, 3.66 Mya. This finding provides strong support to those previous studies which have interpreted the G-1 prints as generally modern in aspect.

Keywords: bipedalism; biomechanics; evolution; hominid; gait

1. INTRODUCTION

The human foot acts primarily to balance the body when standing, and to brake or propel it during gait, although a variable degree of usable grasping and manipulative capacity remains. The former functions occur by exertion of pressures, comprising vertical, transverse and shear force components, against the substrate. Even for modern feet, because of the articular complexity and inaccessibility of the 22 bones and associated layers of soft tissue, nearly a century of analysis has failed to elucidate internal motion, particularly in the midfoot [1]. Further, analyses of the origin and evolution of early hominin foot-function have been based primarily on a limited number of fossils, representing only subsets of the foot skeleton [2]. It is hardly surprising therefore that interpretations of external function in fossil specimens have been contradictory [3,4], with some concluding that there may have been multiple paths to bipedality in the different lineages represented by fossil footbones [5]. Consequently, various authors have turned to footprints and associated trails [6–12] as a more direct line of behavioural evidence—fossil footprints and trackways, although rare in the geological record, are probably more common than articulated fossil footbones.

The best-known early hominin footprint trails are those at Laetoli locality G, Tanzania, dating to

*Author for correspondence (rhcromp@liv.ac.uk).
†These authors contributed equally to this work.

Electronic supplementary material is available at http://dx.doi.org/10.1098/rsif.2011.0258 or via http://rsif.royalsocietypublishing.org.

Received 22 April 2011
Accepted 28 June 2011

3.66 Mya [13], made in nephelinite volcanic ash which is assumed to have been damp at the time of footprint formation [14,15]. Trail G-1 was made by a small individual walking to the left of trail G-2/3, which consists of larger prints made either by one individual whose feet slipped, or two individuals, the second treading in the footsteps of the first [16]. The overlap/slippage in G-2/3 currently precludes meaningful analysis. Functional interpretations of G-1 foot function to date are directly contradictory, arguing either for a generally modern aspect, with a medial longitudinal arch, lateral-to-medial force transfer and push-off by the hallux [6,16]; or that these features are absent and/or foot-function as close or closer to that of non-human great apes [8,17,18]. These contradictions may partly be attributed to difficulties in statistical analysis of footprint morphology, which, consisting of plastic deformation of a substrate under pressures applied by deformable soft tissue, can lack reliable landmarks. Recent quantitative studies of the Laetoli footprints have either assumed that some landmarks exist [10], or limited themselves to single overall parameters of the footprints, e.g. comparing maximum depths under the hindfoot and forefoot [12]. Moreover, while it is generally agreed that footprint depth reflects foot pressure [7–12], it is unknown whether maximal- or time-integrated pressure is more important in substrate deformation [11]. Measurement of pressures transmitted by humans through moist sand [11] suggests that both pressure measures are good predictors of depth but whether maximal pressure or pressure impulse is the better predictor of depth varies with foot region. This is because of complex, nonlinear interactions between foot and substrate [9,11], but cannot be assumed to hold for hominins where forefoot function may not have been closely similar to our own. No means of differentiating the local effects of maximal- and time-integrated pressure in ancient footprints has yet been reported, to the best of our knowledge, and until such a technique has been developed, we can only assume a general equivalence of footprint depth and foot-pressure, *sensu lato*.

In this study, we aimed to provide tests of the two main competing hypotheses, that (i) the G-1 footprints resemble human footprints/foot-pressure records more than they do equivalent records for voluntary bipedalism of non-human apes, in displaying a medial twist of the forefoot on the hindfoot, and thus a medial longitudinal arch, lateral-to-medial force transfer and push-off by the hallux [6,19]; or (ii) that these features are absent, and that the foot-function represented by G-1 thus evinces as much, or closer, affinity to foot-function in non-human apes [8,17,18].

Testing these hypotheses requires that we compare depths over the whole footprint, and to do so, we apply statistical parametric mapping (SPM), a topological technique recently adapted for foot-pressure studies [20] to pixel-by-pixel depth comparison of the mean G-1 footprint to means of human footprints recorded experimentally in the laboratory and in the field. We supplement these by experimental recordings of foot-pressure in the facultative bipedalism of bonobos (pygmy chimpanzees), which have the most human-like limb proportions of the non-human great apes, but use bipedalism in less than 2 per cent of the natural locomotor repertoire, and orang-utans, with less human-like body proportions but 7–8% of bipedalism in their natural locomotion [21,22], and by computer simulations of footprint formation in the most likely author (e.g. [19]) of the Laetoli G trackways, *Australopithecus afarensis*, during alternative hypothesized gaits and assuming alternative mass distributions.

2. MATERIAL AND METHODS

2.1. Sediments

The total depth of the Laetoli G ash fall is 120–150 mm, but this contains two components [15,23]. Within these, prints of giraffids, rhinoceratids and proboscideans are only 20–40 mm deep, indicating the maximum compressibility of the Laetoli sediment under the stresses applied by vertebrate trackmakers [15,23]. At this point, either through densification or more probably as a result of lithification of sub-surface layers into an incompressible state, the substrate was by definition able to bear the applied pressure, supporting the animal's weight and propulsive forces. Strain (and therefore deformation) ceased, despite any continued application of stress; and the dynamic pressure associated with movement of the trackmaker's foot would no longer be reflected in track morphology. In order to compare the Laetoli footprints to familiar modern human footprints, in conditions broadly applicable to those of the Laetoli track-bearing substrate, experimental footprints were made by Western human (i.e. habitually shoe-wearing) subjects walking over a 6 m wooden walkway covered with 3–4 cm of loose dry sand at self-determined 'comfortable' walking speeds while keeping their eyes on a head-height image on a wall at the end of the walkway to avoid targeting. Ad libitum practice was allowed so that subjects could find a start point which resulted in a natural same-foot strike in the centre of the test area, a soft-walled box within the sand, covering a Kistler forceplate/RsScan pressureplate combination, set in the centre of the walkway. Procedures followed (for maximum comparability) the set-up in the most detailed recent study of footprint formation [11]. As in this study [11], the box was filled with *ca* 40 mm of moist (*ca* 20% water content), well-sorted, texturally mature, medium sand (grain size between 0.2 and 0.5 mm) grains generally being well-rounded and of moderate to high sphericity. Similar sands have been reported [6,23] as having consistency similar to that of the Laetoli beds at the time of footprint formation. The depth of *ca* 40 mm chosen for the sand mimics the presence and vertical location of the rheologically incompressible sub-surface layers at Laetoli G-1 [15,23], and would impose limits on sediment deformation and track depth broadly similar to that which appears to have existed through mechanical layering of the sediment at Laetoli. It should be cautioned that footprint formation under these conditions cannot exclude potential influences of the retaining walls. Therefore, in trials where a subject placed their foot

near the edge of the box, the trial was discarded and the subject asked to repeat the trial. Similarly, habitual wearing of footwear will constrain the distribution of foot-pressure [24]. For this reason, a smaller sample of footprints was also recorded in moist sand under less-constrained conditions, made by habitually barefoot subjects from the modern Kenyan village of Ileret.

Experimental prints were laser-scanned at 120 µm resolution with an LDI PS-400. First-generation casts of the Laetoli G-1 prints at the National Museum of Kenya and the modern Ileret experimental sample were laser-scanned using a Konica-Minolta VI900, vertical resolution 90 µm. Scans were selected for completeness and output as point-clouds. Prints G-1/28 and G-1/30 were omitted as excessively eroded and damaged by vegetation; G-1/38 since the posterior-heel imprint is missing through faulting [14].

The scanners were positioned over the footprints as orthogonally as possible to the surrounding surface and orientation checked with a two-axis spirit level. However, there will always be a slight variation in the orientation of the XY plane of the scanner relative to the substrate surface between prints, which could result in error when extracting the print, as thresholding is performed along the Z-axis. Further, footprints may be surrounded by uplift and other artifactual relief [9], and the outline is often particularly affected by disturbance of plant and animal origin [25]. To correct for orientation and uplift errors, a plane was fitted to a number of points on the surface of the substrate in which the print is formed, but well outside the print margin. XYZ values of random points in the laser scan data for the palaeosurface were selected, 5 points on the medial side of the footprint and 5 points on its lateral side. The least-squares coefficient of a plane fitted to the extracted points was calculated, any deviation of this plane from the XY plane of the scanner derived, and the transformation values necessary to correct it calculated. These transformation values were then applied to the original scan data so that the surface lay on the same XY plane as that of the scanner. Prints were then isolated using manual thresholding, and downsampled to 1 mm^2 (100 pixels per square cm) to match pressure-plate pixel density. It is surely unlikely that smaller features would represent substantial gait pressures even in relatively compacted substrates. Pixel depths below the reference surface were the basis of all subsequent analysis. Since perceived outlines of footprints will vary with depth, and as noted above will be affected by uplift of the surrounding area during footprint formation, by bioturbation of the sediment, and by erosion, outlines are not analysed or discussed in this study.

Footprints differ particularly in orientation, within a trackway, in size between individuals, and in shape between species. Therefore, registration was conducted using custom Matlab software that manipulated image location, rotation and scaling to maximize the mutual information between a pair of images. The result was an optimally aligned pair of images, a process replicated for all images. Images were mirrored, preliminarily registered to one of the most detailed prints, G-1/34, pixel-wise mean depth computed and original thresholded images re-registered to the mean. The mean of these images was analysed. Central pressure, and pixel-depth, tendencies were calculated, and samples statistically compared using a topological approach under our custom software [20], pedobarographic statistical parametric mapping (pSPM).

2.2. Pedobarographic statistical parametric mapping

pSPM has adapted the SPM approach [26] developed for cerebral blood flow analysis in functional magnetic resonance imaging and positron emission tomography. While SPM methodology is quite complex, its fundamental purpose is quite simple, that is, to detect changes in blood flow. It achieves this by probing the brain volume to identify regions of significant change topologically. Two important characteristics make this possible: (i) the brain is contained within regular discrete bounds, and (ii) blood flow is spatially smooth. In this paper, we simply substitute footprints for brains, and depth for blood flow. Footprints are also (i) contained in generally regular discrete bounds (the plantar foot shape) and their depths are also (ii) generally spatially smooth across the surface of the foot. As multiple footprints have similar geometry, it implies that the footprints are able to be registered [27] or, equivalently, that they can be spatially manipulated to match a template footprint within a certain error tolerance. Once registered, each pixel corresponds to the same anatomical location in all co-registered images, so standard test statistics (e.g. t, F) can be meaningfully computed at each pixel or voxel. The result is a statistical image or an SPM. However, the value of a test statistic does not, by itself, convey statistical significance. While we could compute p-values for every single pixel in the SPM, we have a major problem. There are tens of thousands of pixels in footprint images, so it is very likely that we will observe large t values (e.g. $t > 3$) simply by chance. Fortunately, the second shared characteristic of footprint and brain images, spatial smoothness, provides us with an elegant and powerful solution to this problem: topology. Since neighbouring pixels tend to behave similarly, their t values also form a generally smooth SPM and it can be shown that the topological characteristics of a thresholded SPM (e.g. cluster size, number of clusters, etc.) follow analytical probability distributions (e.g. [26]). This is profound because the spatial sampling frequency, or equivalently the number of pixels, is irrelevant. What matters is the spatial smoothness of the measured signal. Thus, SPM transcends classical multivariate statistics by moving completely into the realm of topology. Indeed, it can be shown that SPM constitutes a generalization of univariate statistics to n-dimensional spatio-temporal data and that SPM's topological approach can be used to analyse a wide variety of spatio-temporal biomechanical data [28].

A sceptic might argue that SPM is unnecessarily complex: one could manually identify different landmarks or regions of interest (ROI) over the foot, and then conduct statistics within each ROI, or incorporate ROI data into multivariate analyses, and arrive at a similar answer to that yielded by SPM procedures. We would counter by suggesting that SPM, or

something similar, is necessary for objective analysis. Manual ROI identification inevitably involves qualitative judgement, but even when it is highly repeatable [29] more serious problems emerge: the selected ROIs may miss or distort functionally relevant signal [20,28]. Thus, ROI definition, as a general methodology, constitutes an *ad hoc*, incomplete and potentially biased approach that cannot be guaranteed to assess accurately the underlying spatio-temporal trends of smooth surfaces. We therefore argue that SPM offers three main benefits for footprint analyses: (i) it is objective, (ii) it assesses the entire spatial domain and (iii) it is not susceptible to problems of *ad hoc* ROI discretization.

2.3. Foot pressure in bipedal walking of non-human great apes

Foot pressure in voluntary, unelicited bipedalism of bonobos was recorded in a large island enclosure at Planckendael Zoo, at a resolution of 16 pixels cm^{-2}, using RSscan Footscan 0.6 m pressure plates set in a wooden walkway. Records were also made of a juvenile orang-utan at Twycross Zoo walking over a 1 m Footscan plate with the same resolution, placed on a rigid floor. The orang-utan was guided by its habitual keeper by a light hand-touch, the keeper being requested to provide no support. Only records where no support was evident were retained for analysis. All such work was approved by zoo authorities in advance and adhered strictly to the ASAB/ABS Guidelines [30].

2.4. Computer simulations

Forward-dynamic models used in the computer simulations followed previous procedures [31]: briefly, skeletal models derived from measurements of AL-288-1 and other *A. afarensis* specimens, taken from the literature, were rigged with simulated lower limb muscles [32] with Hill-type properties, incorporating both parallel and serial elastic elements. The model was assigned alternatively chimpanzee-like or human-like mass distribution, human values being those previously [31] taken from the standard anthropometry literature [33] and chimpanzee values obtained from segmented specimens using a variant of the complex-pendulum technique [34]. While three-dimensional, the model was constrained to the sagittal plane to avoid lateral instability. Gait was generated using a finite-state feed-forward controller and genetic-algorithm optimization was used to minimize metabolic cost of locomotion for each gait type/model combination in a process analogous to natural selection [31]. The feet were rigid with spring-damper contacts at the heel and metatarsal heads modelling ground contact. Foot-pressure distribution was generated by summing impulses transmitted through each contact. Both 'bent-hip, bent-knee' (BHBK) and erect gaits were generated by random changes in the muscular activation genome and the most efficient of these were retained for the next 2000 plus iterations required to identify stable optima [31].

3. RESULTS

Qualitative comparison (figure 1) of normalized means for the three-dimensional morphology of G-1 and experimental footprints made in moist sand by Western humans (see also electronic supplementary material, figures S1, S5, S6 and movie S1) indicates several similarities: (i) the heel impression is substantially deeper than that of the forefoot; (ii) there is a continuous depression under the region of the metatarsal heads across the whole width of the foot; (iii) there is a raised area under the medial midfoot area, which does not extend into the lateral midfoot (see also electronic supplementary material, movie S1); and (iv) there is a clear impression under the hallucal phalanges. Direct statistical comparison of manually registered Western and G-1 means (figure 2 and electronic supplementary material, figure S2) shows that significant differences nevertheless exist (even though mean footprints for different modern human individuals differ substantially in, e.g. depth under the hallux and the position and extent of the maximum depth under the metatarsals). In the Western human mean: (i) the impression in the area of the human medial longitudinal arch is shallower and more extensive; the midfoot impression is narrower and its lateral margin shallower; (ii) the impressions of the hallucal phalanges are moderately deeper; (iii) the hallucal metatarsal and central-toe regions are somewhat deeper; (iv) the rear heel impression is somewhat deeper; and (v) the impression under the lateral margin of the foot is shallower. Consequently, the G-1 prints differ in the extent of expression of several functionally related characteristics from those made by modern human feet of habitually shod individuals. However, the most appropriate comparator for the G-1 print-maker must be habitually barefoot humans, and indeed some distinguishing features of the G-1 mean are recalled in published foot-pressure records [24] and a small sample of footprints (electronic supplementary material, figure S7) for habitually barefoot individuals: toes are somewhat fanned-out; depths and hence foot-pressure maxima are more diffuse; the midfoot impression is broader and the elevation in the medial longitudinal arch region is less marked. SPM requires a sufficiently high level of geometric similarity between images to allow registration. G-1 footprints, like modern human footprints and pressure records, are sufficiently consistent step-to-step, to allow registration within-species, and close enough to those of humans to allow registration between-species. However, there is high inter-step variability in pressure recordings of bonobo and orang-utan bipedalism (figure 3*a,b* and electronic supplementary material, figures S8 and S9). While bonobo and orang-utan records could be registered intra-species, shape/scale differences from both the G-1 mean and multi-subject means for human footprint records precluded registration, so that we can only make the qualitative observation that distinctions from G-1 and human footprint means are very substantial: particularly in the *combination* of evidence for more consistent placing and intensity of hallucal phalanx contact, greater medial extent and intensity of metatarsal head contact, and greater shallowness

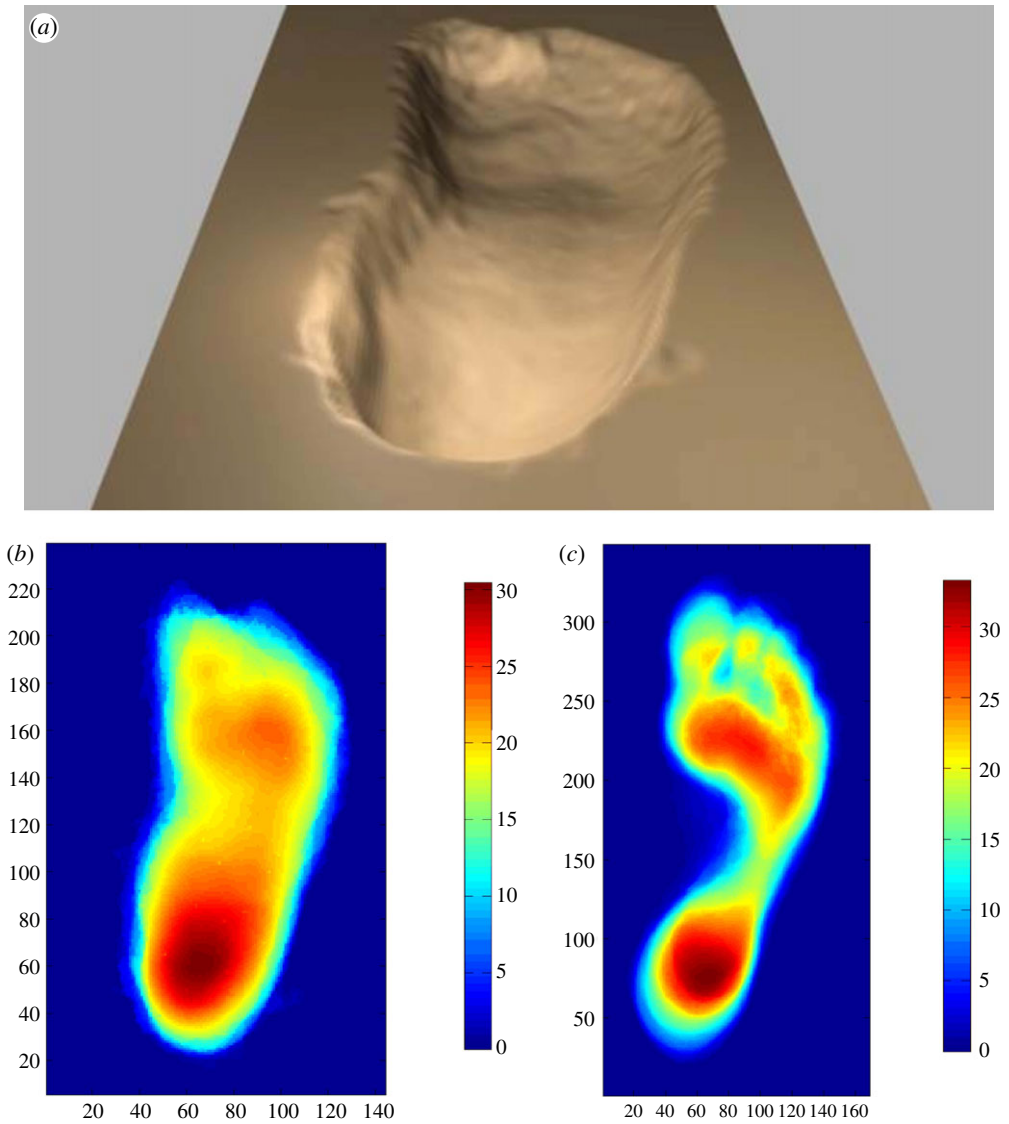

Figure 1. Central tendency of footprints. (*a*) Laetoli G-1 mean in perspective. (*b*) Laetoli G-1 mean as greyscale depth map ($n = 11$). (*c*) Habitually shod human mean as greyscale depth map (five male and five female adults, 10 trials each) walking in moist fine-sand. (*b*,*c*) Black areas indicate *XY* reference plane. Darker shades within the 'footprints' indicate greater mean depth. Dimensions in millimetre; resolution 1 mm^2. (False-colour plots in electronic supplementary material, figure S1, individual records in false colour in electronic supplementary material, figures S5 and S6.) (Online version in colour.)

and extent of shallow impressions under the medial midfoot. But, treating pressure and depth as equivalent, we did succeed in the manual registration of a remarkable single print of a habitually barefoot individual from the modern village of Ileret, walking normally and apparently asymptomatically (figure 3*c*), to the bonobo mean (figure 3*d*–*f*). We also registered it to the G-1 mean (electronic supplementary material, figure S10*a*,*b*) and subsequently subtracted the registered images (electronic supplementary material, figure S10*c*). It differs from the G-1 mean, but resembles the bonobo pressure mean, in showing a double-peaked impression in the lateral midfoot, actually deeper than that for the heel, very limited medial extent and intensity of metatarsal head contact, and a very weak hallux impression. Of course, this single print may be atypical of even this individual, but it seems to suggest that the G-1 mean lies within the range of asymptomatic variation of human footprints. This interpretation is further suggested by a similar phenomenon in a published pressure record (fig. 1*b* in Crompton *et al.* [35]) from normal walking of another apparently asymptomatic African individual, and such a pattern is apparently common in some African populations (J.-P. Wilssens 2005, personal communication to K. D'Août). We do not have information on the foot morphology of these individuals, but have since identified a similar feature in some habitually shoe-wearing, asymptomatic individuals of British origin for whom we have collected pressure-treadmill records (see e.g. electronic supplementary material, figure S10*d*), and are currently analysing internal hard and soft tissue morphology of their feet using ultrasound.

Figure 4 shows predicted pressure under a simplified foot for our forwards-dynamic simulations of upright and BHBK gait (see also electronic supplementary material, figure S4). Irrespective of mass distribution, higher pressure occurred under the hindfoot in upright walking, but under the forefoot in BHBK walking. Using stature, rather than the more usual hip height,

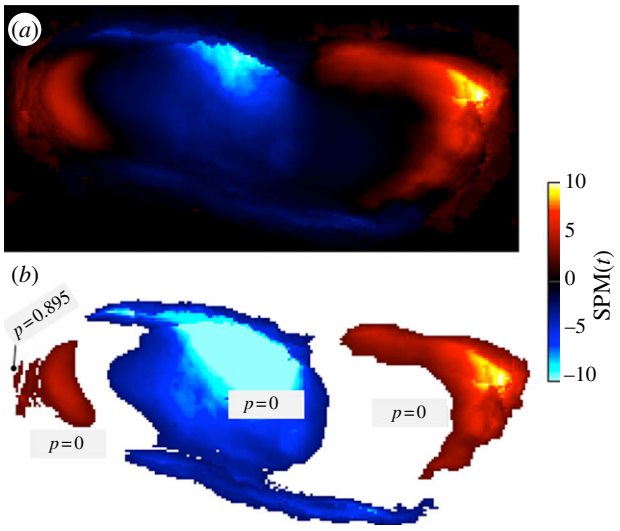

Figure 2. Statistical comparison of G-1 and habitually shod human footprints. Heel is to left, toe to right, medial above and lateral below in each plot. Black or white outside 'prints' indicate XY reference plane, inside 'prints', regions of no difference. Brighter areas indicate larger differences. (a) Raw statistical parametric map (SPM(t)), constructed from pixel-level t-tests. Lighter regions indicate where the means differ most. (b) Thresholded inference image (height threshold $t > 2.5$, cluster-size threshold 10 pixels) showing topological significance p of the immediately adjacent suprathreshold clusters. Significance of the t-values is greatest under the medial midfoot, hallux and anterior heel. Dimensions normalized by registration. (False colour maps in electronic supplementary material, figure S2.) (Online version in colour.)

to derive Froude numbers (loosely, dimensionless speed, following Alexander [36]), we obtained values of approximately 0.35 for optimized BHBK simulations, and 0.24 for optimized erect simulations. The stride lengths in the optimized BHBK simulations were 1.44 and 1.53 m for chimpanzee-like and human-like mass distribution simulations, respectively, and for optimized erect walking, 0.76 and 0.85 m for the chimpanzee-like and human-like mass distribution simulations, respectively.

4. DISCUSSION

4.1. Effects of speed on footprint depth and morphology

A study [36] of walking speeds represented by the Laetoli trails (using Froude numbers calculated from stature) gave values ranging from 0.17 to 0.2. In comparison, a 'small town' human walk tends to occur at a stature-based Froude number of 0.2, and a 'big city' walk at 0.4 [37]. The self-selected/comfortable treadmill speed for level walking has a stature-based Froude number of 0.34 in humans [38]. The values previously estimated for Laetoli [31,36] and those produced by optimization of the current computer simulations are thus all medium/comfortable walking speeds for individuals of similar stature/limb length. Walking speed in our footprint creation experiments was chosen on the basis of the earlier estimates [29,34]. On the basis of our experimental studies of human foot pressure [39], higher speeds would tend to produce higher pressures under the forefoot and hindfoot, and lower pressures under the medial midfoot. Slow walking would tend to produce the reverse. We expect that the same will be shown to apply to footprint depths, and pilot studies follow this expectation.

4.2. Effects of body mass on footprint depth and morphology

The Laetoli hominins were probably lighter as well as shorter than most modern humans. However, we consider this is unlikely to influence footprint form. Firstly, we are comparing not absolute depths but depth distributions. Secondly, the mass of a subject, is transmitted to the substrate as pressure, i.e. mass/foot area. There exist relatively little data on how plantar foot area scales with body mass, but within confidence limits, scaling has been found to be isometric in both those reptiles [40] and those mammals [41] so far studied. Therefore, it seems reasonable to assume *pro tem* that mass/foot area was broadly similar to that in humans, and that mass differences are unlikely to exert much effect on relative depth distributions within footprints.

4.3. Effects of moisture on footprint depth and morphology

A previous study using experimental footprint formation to interpret the Laetoli footprint trail [12] used sand with at most half the moisture content, but greater sand depth to our study. Our choice of 40 mm depth of sand is a more accurate mimic of the sedimentological conditions of Laetoli G because of the existence of rheologically incompressible layers in the Laetoli G stratigraphy at an equivalent relative depth [15,23]. Further, pilot studies showed that for the type of sand we used, 20–30% moisture content was optimal for retention of detail combined with reasonable footprint depth. Below 20 per cent, areas of the footprint (especially under the metatarsal heads) tend to fragment, and above some 40 per cent, greater moisture does not increase print depth. Increasing moisture content initially decreases sediment strength. As the proportion of water increases, the pores fill with water, reducing sediment strength as grain-to-grain interactions become facilitated and lubricated, allowing more plastic deformation to occur. However, soil mechanics considerations [42] indicate that for any given sediment particle-type, a point will be reached where the incompressibility of water offsets its lubricating effect, and the sediment becomes less readily deformable.

4.4. The functional characteristics of the Laetoli footprint maker

4.4.1. Facultative or habitual bipedality? Early hominins are often presumed to be uncommitted or facultative bipeds. Comparison of figures 1 and 3 (and of electronic supplementary material, figures S1 and S5 with S8 and S9) shows that G-1 prints share with humans a higher degree of inter-step consistency than our bonobo and

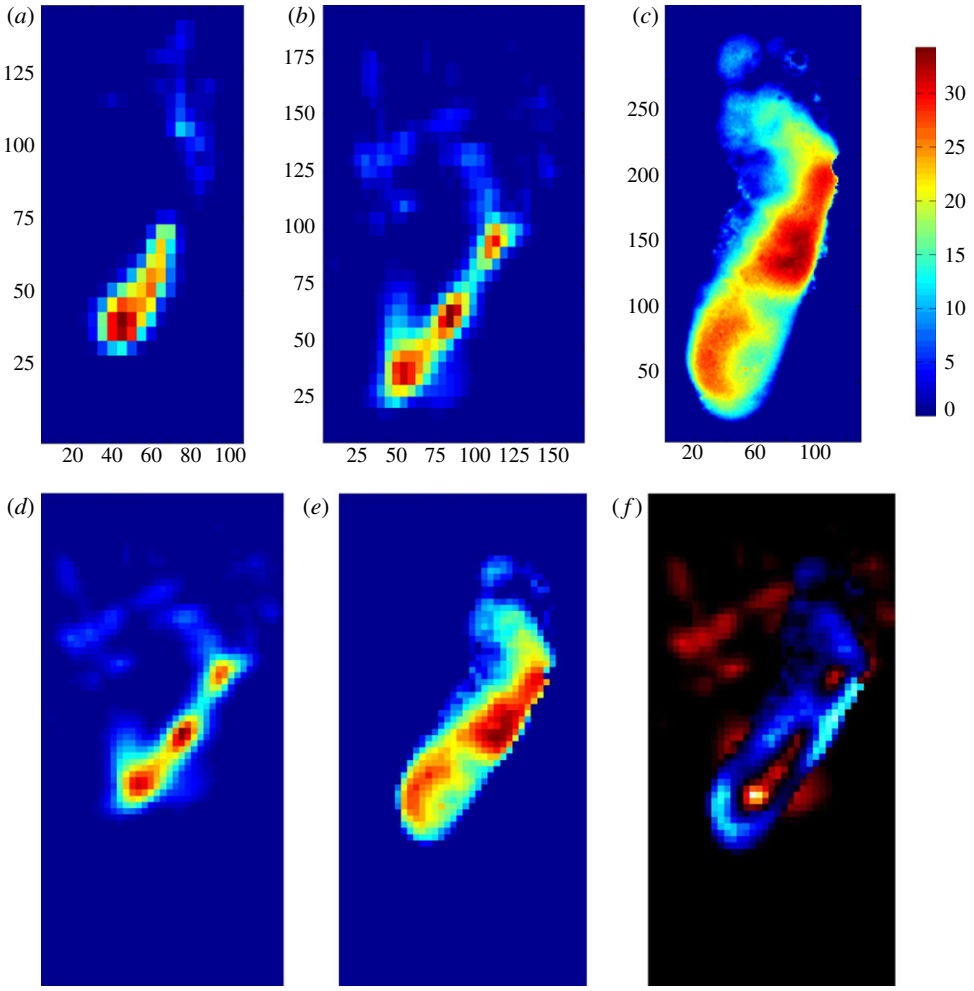

Figure 3. Foot pressure in orang-utan and bonobo bipedalism. Mean peak-pressure for (*a*) elicited bipedalism of a hand-reared orang-utan ($n = 10$); (*b*) voluntary bipedalism of naturally reared bonobos ($n = 11$). Individual records in electronic supplementary material, figures S7 and S8. (*c*) A footprint from a habitually barefoot human from modern Ileret, showing an apparent mid-tarsal break (resolution 1 mm^2). Dimensions in millimetres, pixels 25 mm^2. Darkest areas indicate the zero-data reference plane. Intense pixels within the foot-pressure record or footprint indicate (*a*,*b*) higher relative peak pressures; (*c*) greater relative depth. Light pixels to upper left of (*a*) and (*b*) are made by hallux, and indicate low pressure and highly variable posture. Intense pixels within the pressure record in (*a*) and (*b*): bottom, heel-region maximum, middle: mid-tarsal maximum, top: lateral-metatarsal maximum. (*d*) Bonobo mean pressure; (*e*) Ileret footprint, after manual registration with (*d*); (*f*) subtraction of (*d*) and (*e*). In the subtraction, dark surround indicates no difference, dark areas 'inside' the 'print' indicate areas of no difference, brighter areas indicate stronger differences. Dimensions normalized by registration. (False colour maps in electronic supplementary material, figure S3.) (Online version in colour.)

orang-utan records. Inter-step consistency is strongly suggestive of habitual bipedality in the G-1 printmaker.

4.4.2. Upright or bent hip, bent-knee gait? Living African apes apart from ourselves usually employ BHBK gait in their facultative bipedalism. Some have argued [17,43] that *A. afarensis* would have similar gait either as a result of considerable arboreality [17] or as a transition from knuckle-walking quadrupedalism in a purportedly chimpanzee-like common ancestor of humans, chimpanzees and bonobos [43]. However, BHBK gait is mechanically inefficient, because of muscular work required to stabilize the joints' posture against gravity [44], and would result in increased forefoot pressures, because of ankle dorsiflexion at touch-down [45]. It might be argued that the ankle would not have dorsiflexed at touchdown in the G-1 printmaker, because of differences from humans in body-build. Our computer model of *A. afarensis* shows that optimized BHBK gaits with chimpanzee-like or human-like mass distribution do indeed both have the same dorsiflexed ankle posture at touch down, leading to near-simultaneous full-foot, or forefoot touchdown (electronic supplementary material, movies S2 and S3). However, in both erect walking simulations, the heel contacts first (electronic supplementary material, movies S4 and S5). Further, in the BHBK gait, the line of action of the centre of mass lies behind the knee, but in front of the ankle [45] (electronic supplementary material, movies S2 and S3). Both characteristics will increase forefoot pressure relative to hindfoot pressure and thus predict deeper forefoot impressions and reduced hindfoot impressions. Our present three-dimensional Laetoli G-1 mean data

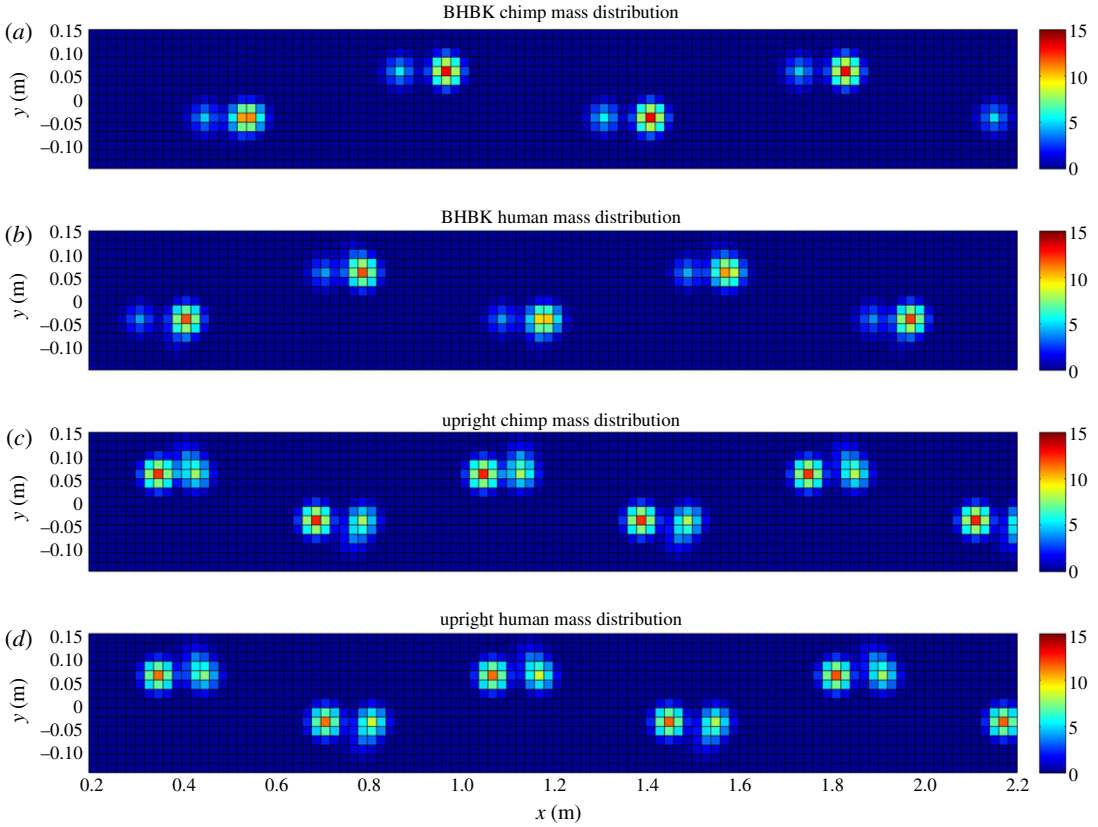

Figure 4. Predicted foot pressure in alternative simulated *A. afarensis* gaits. Predicted foot pressure (impulse, Ns, over 40 mm^2 areas) from a simulation of *A. afarensis* in: (*a*,*b*) BHBK gait; (*c*,*d*) upright gait. (*a*,*c*) Results with chimpanzee-like mass distribution; (*b*,*d*) with human-like mass distribution. Dark areas 'outside' the 'prints' indicate the zero-data reference plane, dark areas within the 'prints' the highest predicted pressure, lighter areas lower pressure. (False colour maps in electronic supplementary material, figure S4.) (Online version in colour.)

(figure 1) show that heel impressions are substantially deeper than forefoot impressions, as predicted by both our *A. afarensis* simulations of erect walking.

As previously stated, our three-dimensional laser scans were at millimetric resolution, and pixel depth was measured with reference to a plane fitted to 10 random points on the land-surface well outside the footprint margin. Sloping of the original land-surface might introduce a potential bias in relative depths of the heel and toe impressions, and indeed the Laetoli G area shows a 2° dip [23]. Nevertheless, when we adjusted print orientation to allow for different up- and downslopes, disparity in heel versus toe depth was not eliminated until we adjusted print orientation to allow for 15 per cent (8.53°) upslope of the G-1 sediments (electronic supplementary material, figure S11). However, a previous attempt [12] to test whether the Laetoli G-1 printmaker walked erect, or BHBK by comparing experimental footprints for humans walking erect and BHBK in sand, suggested that the G-1 footprints had near-equal heel and toe depths. The average absolute footprint depths presented in this previous study [12] are four times greater than the mean depths we obtained from carefully aligned laser scans of the original casts. The cause of this discrepancy between our work and the previous paper [12] is difficult to assess as the latter provides limited explanation of the derivation of absolute heel and toe depth values from the contour plots in the (Leakey and Harris) Laetoli monograph, and of the location, orientation and derivation of the reference plane from which their depth values were measured, so that it was impossible to reproduce their calculations. We reiterate that our plotted depth values are calculated with reference to a plane fitted to 10 points on the scanned palaeosurface well outside the print outline or any associated push-up structure. The previous study [12] gave raw mean heel-depths and mean toe-depths of 124.94 and 131.65 mm, respectively, and, after adjustment for a stated but unreferenced 3° upslope of the G locality, mean toe depth of 125.05 mm. These absolute depths would place the palaeosurface above the level of an adult human ankle joint. Indeed, the peak corrected toe depth given, 195.8 mm, is in excess of the 120–150 mm total depth of both units of the Laetoli Footprint Tuff. We can only assume that when the authors state that only relative depths are important, they are calculating depths relative to a hypothetical reference plane located well above the level of the palaeosurface [12]. Our measured depths are compatible with the published depths of the Laetoli Footprint Tuff ashfall units above the incompressible sub-layers [15,23]. Given that approximately 15 per cent upslope is required to produce equal heel and toe depths using our data and methodology, we are confident that our results therefore provide more definitive and unequivocal evidence that an efficient, upright gait was employed by the Laetoli printmaker.

4.4.3. A mid-tarsal break? One of the first functional distinctions to be reported between the feet of humans and of other apes was the deduction from footprint form that chimpanzees exert pressure on the substrate under the lateral foot between the heel and the metatarsal heads, by flexion of the midfoot, whereas humans do not ([46], and reviewed in [47]). The case in humans was attributed to so-called 'locking' of the transverse tarsal joint (comprising the joints between talar head and navicular medially, and calcaneus and cuboid laterally), and thought to result from the mid-tarsal region (midfoot) acting as a rigid lever, that transfers force more effectively during push-off (reviewed in [47]). It is now generally held [2,5] that any 'locking' mechanism in humans is substantially attributable to a larger and more eccentrically placed peg or flange projecting from the cuboid into a corresponding groove on the calcaneus. This feature is unique to humans among primates, although plantar ligaments are also thought to contribute to the resulting midfoot stiffness [47]. Consequently, arguments that the Laetoli G-1 footprints are 'ape-like' rather than 'human-like' depend, in part, on whether there is evidence for a pressure peak under the midfoot, suggesting mid-foot dorsiflexion and a mid-tarsal break. At least two papers [7,8] have claimed, on the basis of subjective interpretations of features of individual prints, that this is indeed the case.

The foot-pressure records shown in figure 3 and electronic supplementary material, figures S8 and S9 appear to be the only statistically adequate published samples of foot pressures in bipedal walking of non-human great apes. Composite pressure records for common chimpanzees [48] do not differ substantially from the present results and a single record of lowland gorilla foot pressure (electronic supplementary material, figure S12) and large samples of foot pressures in bipedalism of gibbons [49] again follow the general patterns reported here in bonobo and orang-utan. Single- or double-pressure peaks under the lateral midfoot, suggesting a mid-tarsal break, are evident in all of them. The Laetoli G-1 mean lacks any feature suggestive of a mid-tarsal break.

However, while it has long been understood that the human medial midfoot is very mobile, a recent study using bone-pins suggests [50] that the human lateral midfoot is also much more mobile than previously thought. While humans may not attain the *ca* 28° of total lateral midfoot dorsiflexion apparently seen in bonobos [51,52], the total range of motion in the small experimental sample of six individuals was considerably greater than the traditional concept of a stiff human lateral midfoot might suggest, summing to 33° at the two contributing joints (calcaneocuboid and cuboid–fifth metatarsal). A high degree of variability was evident [50] in much of the lateral midfoot: for example, while some subjects showed substantially greater mobility at the calcaneocuboid than the cuboid-fifth metatarsal joint, others showed the reverse. Further, we have observed that footprints and pressure records from some human individuals, both habitually barefoot and habitually shod, do show lateral midfoot pressure peaks, demonstrating lateral midfoot weight bearing (e.g. figure 3*c*, electronic supplementary material, figs 10*d* and 1*b* in Crompton *et al.* [35]). These might result from a particularly salient fifth metatarsal tuberosity, but equally or additionally might suggest substantial dorsiflexion at the joints between calcaneus and cuboid, and cuboid and fifth metatarsal; and the latter seems more likely when two lateral midfoot peaks are apparent, as is the case in figure 3*c*.

4.4.4. A medial longitudinal arch? Footbone morphologies of *A. afarensis* [17], *H. habilis* [53] and even *H. floresiensis* [2] have been widely interpreted as suggesting an unstable or incompletely stabilized midfoot unable to sustain a medial longitudinal arch: such interpretations often rely substantially on whether or not a human-like cuboid peg is present. Lack of a medial arch implies lack of capacity to store energy in plantar tissues, a major factor increasing the efficiency of human gait [54].

Figure 1 shows a clear elevation under the medial midfoot of the G-1 mean, which is even more evident in a rendered three-dimensional animation (electronic supplementary material, movie S1). Subtraction of the registered G-1 and human means (figure 2) shows that the elevation is lower and of lesser extent than the mean in modern habitually shod humans. Qualitative comparison of the G-1 mean with mean foot-pressures in bipedalism of bonobos and orang-utans (figure 3*a,b* and electronic supplementary material, figures S8 and S9) shows that while an unloaded area exists under the medial midfoot of the non-human apes that we have studied, this is not combined with evidence for a hallucal toe-off and elevated pressure under the metatarsal heads, as in most humans and the G-1 hominin. Rather this unloaded area under the medial midfoot in bonobos and orang-utans is correlated with clear pressure peaks under the lateral midfoot, indicating plantar collapse, and hence push-off [22] at the proximal and/or distal articulations of the cuboid. Our evidence strongly supports the view [3,19] that the G-1 prints attest to a functional medial longitudinal arch in at least the G-1 printmaker, if not their species as a whole. Nevertheless, various papers have argued that anatomical features in *A. afarensis* skeletal elements, including a large navicular tuberosity [5] and a well-marked peroneal groove on the fibular malleolus [55] are evidence that the medial midfoot of *A. afarensis* was weight-bearing, and thus that the species lacked transverse arches and/or a medial longitudinal arch. A two-dimensional analysis of articular orientations [56] also came to the same conclusion. However, a recent paper [51] argues that the form of a new fourth metatarsal of *A. afarensis* indicates, contrariwise, that this species did indeed have a medial longitudinal arch and lacked a mid-tarsal break. Equally, however, another recent contribution [57] argues that the available footbones of the 'Lucy' AL-288-1 individual of *A. afarensis* suggest that this individual was asymptomatically flat-footed, noting correctly that modern humans are highly variable in medial arch height. We may legitimately conclude from this debate that we do not yet understand the relationship

between the bony morphology of the midfoot and its internal kinematics and external function [1].

4.4.5. The species identity of the Laetoli G-1 printmaker. Most authors regard *A. afarensis* as the species most likely to have been responsible for the Laetoli G trackways. However, some regard the G-1 prints as too humanlike for authorship to be attributed to *A. afarensis*, and as no other species is known from Laetoli at the time of deposition of the Footprint Tuffs, suggest that a yet undiscovered hominin more similar to *Homo* was responsible [58]. As figure 3*c–f* shows, some humans can produce footprints similar in several respects to those of some bipedally walking non-human apes. It remains to be demonstrated that the curved lateral toe-bones and distinct hallucal morphology [59] of non-human apes and of *A. afarensis* [17] somehow prevents them from producing footprints within the human range (with the possible exception of consistency of hallux placement), and we should note that some great apes do display everted foot posture (see e.g. electronic supplementary material, figure S12) as well as upright gait. We have shown that there is overlap in foot pressure distribution and footprint form, between living (and even more, fossil) hominins and non-human apes, which implies that there is also an overlap in species' ranges of variation in midfoot kinematics. We agree with the argument [19] that markings supposedly indicating curled toes in some G-1 prints [17] are probably artefactual; they are certainly not evident in the G-1 mean, and, for the present, we see no reason not to attribute the G-1 trail to *A. afarensis*.

Whatever the case in other individuals of the same species, and assuming that the G-1 trackway was typical of its maker, this study demonstrates the absence of a mid-tarsal break in the G-1 trackway. This indicates that, at least during G-1 formation, accelerative force was delivered by the forefoot in the Laetoli trackmaker. Delivering accelerative forces from the forefoot indicates increased gear ratio [60] compared to that indicated by the presence of a mid-tarsal break in non-human ape foot-pressure records and the available great-ape force-plate records. In humans at least, high gear ratios in late stance allow the plantarflexors to operate within the high-efficiency/high-power region of their force–velocity curve near toe-off [60]. On the other hand, we have seen that foot pressure and foot-print records of some humans, as well as other apes, display what appears to be a mid-tarsal break. In the one such case where the path of the centre of pressure (CoP) is also available (fig. 1*b* in Crompton *et al.* [35]), the classic human pattern of lateral-to-medial transfer of the CoP across the metatarsal heads is lacking. The CoP takes a more or less directly forward path, and (fig. 1*c* in Crompton *et al.* [35]) vertical ground reaction forces (vGRFs) decline slowly from a single peak in mid-stance, as in non-human ape bipedalism, rather than rising to a second peak just before toe-off and then declining very sharply, as do normal human vGRFs for 'comfortable' and 'fast' walking speeds [61]. The clear hallux marking evident in the Laetoli G-1 mean, and the continuous impression across the whole of the metatarsal heads, indicates that lateral to medial force transfer did occur, and that toe-off force was delivered by the medial forefoot. If the elevated region under the medial midfoot is not evidence of a medial longitudinal arch, it can only have been formed by aft-shear brought about by the hallux and medial forefoot. However, although the G-1 mean samples only one individual, subtraction of G-1 from the modern Western human mean (figure 2, and see electronic supplementary material, figure S6 for variation) shows a shallower hallux impression in G-1 combined with a less extensive region of low pressure under the medial midfoot, but deeper imprints under the lateral margin of the foot. This suggests that hallucal toe-off force was lower than in humans, making a hallucal origin for the elevation under the medial midfoot less likely, but increasing the likelihood that a medial longitudinal arch was indeed present. In either case, human-like medial twisting of the medial forefoot on the midfoot [62], facilitating lateral-to-medial force transfer, might have been less marked than in ourselves, and perhaps early African *Homo erectus* such as the likely maker of the Ileret [10] prints. However, a full understanding of the functional characteristics of the Ileret prints awaits their pixel-wise statistical comparison with the Laetoli prints and to those of humans, and requires a more comprehensive analysis of the influence of substrate properties on footprint form, as they are likely to have been made in much moister sediments than those at Laetoli.

We have recently shown that in humans, early [63], as well as late [64] in the stance phase, the plantar aponeurosis acts to stiffen [39] and support the plantar foot, and that the forces it exerts increase not only with speed but also latero-medially, because of latero-medial increase in the dimensions of the metatarsal heads [63]. Similar latero-medial increase in dimensions was present in *A. afarensis* AL-333 [65]. Consequently, if *A. afarensis* had a plantar aponeurosis, as is considered the case in *Paranthropus* [66], a functional medial longitudinal arch could have been sustained by such an extended windlass mechanism even before the evolution of bony stabilization of the midfoot by a modern human-like cuboid peg or other bony features. Bony evidence for powerful tibialis posterior and peroneus muscles in AL-333 [5,55] might then be seen as indicating a second, muscular, soft-tissue contribution to arch stiffness. As hallucal toe-off was apparently weaker in the G-1 individual than in humans, but the AL-333 hallucal metatarsal robust, it may well be the case that selection for control of foot compliance, via a medial longitudinal arch supported by an extended windlass mechanism, drove increased hallucal robusticity as much as did an increased stabilization role for the hominin hallux, as traditionally proposed [5]. Nevertheless, we emphasize that we should expect even more functional variation in the extinct species responsible for the G-1 prints than we see in humans, given a relatively high level of inter-stride variability.

Thus, a predominantly objective analysis of the Laetoli G-1 footprints confirms that at 3.66 Mya, the Laetoli G-1 printmaker showed most of the features of external function of the foot seen in modern humans,

albeit expressed to a lesser degree and very likely implemented by a different internal bony morphological configuration. Walking was certainly erect, and external function of the foot was probably characterized by a functional longitudinal medial arch, lateral-to-medial force transfer and toe-off force delivered by a consistently placed hallux, the *combination* of which at least is very unusual, if not absent, in any living non-human ape. Remarkably, variability in modern human foot-pressure records and footprints suggests that mean morphology of the 3.66 million year old G-1 prints may lie well within the range of asymptomatic modern-human variation.

Procedures approved by University of Liverpool Research Ethics Committee (approval RETH 000088).

This research was funded by The Leverhulme Trust and The Natural Environment Research Council, UK. We thank Dr Emma Mbua of the National Museum of Kenya for permission to scan first-generation casts of the Laetoli G-1 footprints; Dr Jack Harris (Rutgers University) and staff and students of the Koobi Fora Field School for assistance in collecting the modern Ileret footprint data, Chester and Planckendael zoos for observational access to the great apes in their care, Drs Ronald J. Clarke and Craig Feibel for advice on Laetoli taphonomy, and the editor and anonymous referees for helpful and stimulating comment.

REFERENCES

1 Wolf, P., Stacoff, A. & Stüssi, E. 2004 Modelling of the passive mobility in human tarsal gears: implications from the literature. *The Foot* **24**, 23–34. (doi:10.1016/j.foot.2003.09.002)
2 Jungers, W. L., Harcourt-Smith, W. E. H., Wunderlich, R. E., Tocheri, M. W., Larson, S. G., Sutikna, T., Awe Due, R. & Morwood, M. J. 2009 The foot of *Homo floresiensis*. *Nature* **459**, 81–84. (doi:10.1038/nature07989)
3 Day, M. H. & Napier, J. R. 1964 Fossil foot bones. *Nature* **201**, 969–970. (doi:10.1038/201969a0)
4 Kidd, R. S., O'Higgins, P. & Oxnard, C. E. 1996 The OH8 foot: a reappraisal of the hindfoot utilizing a multivariate analysis. *J. Hum. Evol.* **31**, 269–291. (doi:10.1006/jhev.1996.0061)
5 Harcourt-Smith, W. E. H. & Aiello, L. C. 2004 Fossils, feet and the evolution of human bipedal locomotion. *J. Anat.* **204**, 403–416. (doi:10.1111/j.0021-8782.2004.00296.x)
6 Day, M. H. & Wickens, E. H. 1980 Laetoli Pliocene hominid footprints and bipedalism. *Nature* **286**, 385–387. (doi:10.1038/286385a0)
7 Meldrum, D. J. 2004 Fossilized Hawaiian footprints compared with Laetoli Hominid footprints. In *From biped to strider* (eds D. J. Meldrum & C. E. Hilton), pp. 63–84. New York, NY: Kluwer.
8 Meldrum, D. J., Lockley, M. G., Lucas, S. G. & Musiba, C. 2011 Ichnotaxonomy of the Laetoli trackways: the earliest hominin footprints. *J. Afr. Earth Sci.* **60**, 1–12. (doi:10.1016/j.jafrearsci.2011.01.003)
9 Allen, J. R. L. 1997 Subfossil mammalian tracks (Flandrian) in the Severn estuary, S.W. Britain: mechanics of formation, preservation and distribution. *Phil. Trans. R. Soc. Lond. B* **352**, 481–519. (doi:10.1098/rstb.1997.0035)
10 Bennett, M. R. *et al.* 2009 Early Hominin foot morphology based on 1.5-million-year-old footprints from Ileret, Kenya. *Science* **323**, 1197–1201. (doi:10.1126/science.1168132)
11 D'Août, K., Meert, L., Van Gheluwe, B., De Clercq, D. & Aerts, P. 2010 Experimentally generated footprints in sand: analysis and consequences for the interpretation of fossil and forensic footprints. *Am. J. Phys. Anthropol.* **141**, 515–525. (doi:10.1002/ajpa.21169)
12 Raichlen, D. A., Gordon, A. D., Harcourt-Smith, W. E. H., Foster, A. D. & Randall Hass, W. 2010 Laetoli footprints preserve earliest evidence of human-like bipedal biomechanics. *PLoS ONE* **5**, e9769. (doi:10.1371/journal.pone.0009769)
13 Deino, A. 2011 $^{40}Ar/^{39}Ar$ dating of Laetoli, Tanzania. In *Paleontology and dating of Laetoli: human evolution in context. Geology, geochronology, paleoecology and palaeoenvironment, vertebrate paleobiology and paleoanthropology* vol. 1, (ed. T. Harrison), pp. 77–97. The Netherlands: Springer Science + Business Media.
14 Leakey, M. D. 1987 The Hominid footprints: introduction. In *Laetoli: a Pliocene site in Northern Tanzania* (eds M. D. Leakey & J. M. Harris), pp. 490–496. Oxford, UK: Oxford University Press.
15 Barker, D. S. & Milliken, K. L. 2008 Cementation of the Footprint Tuff, Laetoli, Tanzania. *Can. Mineralogist* **46**, 831–841. (doi:10.3749/canmin.46.4.831)
16 Agnew, N. & Demas, M. 1998 Preserving the Laetoli footprints. *Sci. Am.* **279**, 43–55. (doi:10.1038/scientificamerican0998-44)
17 Stern, J. T. & Susman, R. L. 1983 The locomotor anatomy of *Australopithecus afarensis*. *Am. J. Phys. Anthropol.* **60**, 279–317. (doi:10.1002/ajpa.1330600302)
18 Deloison, Y. 1991 Les australopithèques marchaient-ils comme nous? Origine(s) de la bipédie chez les Hominidés. (eds B. Senut & Y. Coppens), pp. 177–186. Paris, France: CNRS.
19 White, T. D. & Suwa, G. 1987 Hominid footprints at Laetoli: facts and interpretations. *Am. J. Phys. Anthropol.* **72**, 485–514. (doi:10.1002/ajpa.1330720409)
20 Pataky, T. C., Goulermas, J. Y. & Crompton, R. H. 2008 A comparison of seven methods of within-subjects rigid body pedobarographic image registration. *J. Biomech.* **41**, 3085–3089. (doi:10.1016/j.jbiomech.2008.08.001)
21 Thorpe, S. K. S. & Crompton, R. H. 2006 Orang-utan positional behavior and the nature of arboreal locomotion in Hominoidea. *Am. J. Phys. Anthropol.* **131**, 384–401. (doi:10.1002/ajpa.20422)
22 Crompton, R. H., Vereecke, E. E. & Thorpe, S. K. S. 2008 Locomotion and posture from the common hominoid ancestor to fully modern hominins, with special reference to the last common panin/hominin ancestor. *J. Anat.* **212**, 501–543. (doi:10.1111/j.1469-7580.2008.00870.x)
23 Hay, R. L. 1987 Geology of the Laetoli area. In *Laetoli: a Pliocene site in Northern Tanzania* (eds M. D. Leakey & J. M. Harris), pp. 23–47. Oxford, UK: Oxford University Press.
24 D'Août, K. D., Pataky, T. C., De Clerq, D. & Aerts, P. 2010 The effects of habitual footwear use: foot shape and function in native barefoot walkers. *Footwear Sci.* **1**, 81–94. (doi:10.1080/19424280903386411)
25 Feibel, C. S. 2008 *Microstratigraphy and Taphonomy of Hominid footprints at Laetoli. A Report on the 1995 Field Season*. Report to the Getty Conservation Institute, CA, USA.
26 Friston, K. J., Ashburner, J. T., Kiebel, S. J., Nichols, T. E. & Penny, W. D. 2007 *Statistical parametric*

mapping: the analysis of functional brain images. Amsterdam, The Netherlands: Elsevier/Academic Press.
27 Maintz, J. B. A. & Viergever, M. A. 1998 A survey of medical image registration. *Med. Image Anal.* **2**, 1–37. (doi:10.1016/S1361-8415(01)80026-8)
28 Pataky, T. C. 2010 Generalized *n*-dimensional biomechanical field analysis using statistical parametric mapping. *J. Biomech.* **43**, 1976–1982. (doi:10.1016/j.jbiomech.2010.03.008)
29 Deschamps, K., Birch, I., Mc Innes, J., Desloovere, K. & Matriacali, G. A. 2009 Inter-and intra-observer reliability of masking in plantar pressure measurement analysis. *Gait Posture* **30**, 379–382. (doi:10.1016/j.gaitpost.2009.06.015)
30 Animal Behaviour Society. 2006 Guidelines for the treatment of animals in behavioural research and teaching. *Anim. Behav.* **71**, 245–253. (doi:10.1016/j.anbehav.2005.10.001)
31 Sellers, W. I., Cain, G. M., Wang, W.-J. & Crompton, R. H. 2005 Stride lengths, speed and energy costs in walking of *Australopithecus afarensis*: using evolutionary robotics to predict locomotion of early human ancestors. *J. R. Soc. Interface* **2**, 431–441. (doi:10.1098/rsif.2005.0060)
32 Umberger, B. R., Gerritsen, K. G. M. & Martin, P. E. 2003 A model of human muscle energy expenditure. *Comp. Methods Biomech. Biomed. Eng.* **6**, 99–111. (doi:10.1080/1025584031000091678)
33 Dempster, W. T. 1955 Space requirements of the seated operator. Aerospace Medical Research Laboratory WADC technical report 55/159. Wright-Patterson Air Force Base, OH, USA.
34 Crompton, R. H., Li, Y., Günther, M. M. & Alexander, R. McN. 1996 Segment inertial properties of primates: new techniques for laboratory and field studies of locomotion. *Am. J. Phys. Anthropol.* **99**, 547–570. (doi:10.1002/(SICI)1096-8644(199604)99:4<547::AID-AJPA3>3.0.CO;2-R)
35 Crompton, R. H., Sellers, W. I. & Thorpe, S. K. S. 2010 Arboreality, terrestriality and bipedalism. *Phil. Trans. R. Soc. B* **365**, 3301–3314. (doi:10.1098/rstb.2010.0035)
36 Alexander, R. McN. 1984 Stride length and speed for adults, children, and fossil hominids. *Am. J. Phys. Anthropol.* **63**, 23–27. (doi:10.1002/ajpa.1330630105)
37 Bornstein, M. N. & Bornstein, H. G. 1976 The pace of life. *Nature* **259**, 557–558. (doi:10.1038/259557a0)
38 Minetti, A., Boldrini, L., Brusamolin, L., Zamparo, P. & McKee, T. 2003 A feedback-controlled treadmill (treadmill-on-demand) and the spontaneous speed of walking and running in humans. *J. Appl. Physiol.* **95**, 838–843. (doi:10.1152/japplphysiol.00128.2003)
39 Pataky, T. C., Caravaggi, P., Savage, R., Parker, D., Goulermas, J. Y., Sellers, W. I. & Crompton, R. H. 2008 New insights into the plantar pressure correlates of walking speed using pedobarographic statistical parametric mapping (pSPM). *J. Biomech.* **41**, 1987–1994. (doi:10.1016/j.jbiomech.2008.03.034)
40 Kubo, T. 2011 Estimating body weight from footprints: application to pterosaurs. *Palaeogeogr., Palaeoclimatol., Palaeoecol.* **299**, 197–199. (doi:10.1016/j.palaeo.2010.11.001)
41 Michilsens, F., Aerts, P., Van Damme, R. & D'Août, K. 2009 Scaling of plantar pressure in mammals. *J. Zool.* **279**, 236–242. (doi:10.1111/j.1469-7998.2009.00611.x)
42 Craig, R. F. 1974 *Soil mechanics*. London: Van Nostrand Reinhold.
43 Raichlen, D. A., Pontzer, H. & Sockol, M. D. 2008 The Laetoli footprints and early Hominin locomotor kinematics. *J. Hum. Evol.* **54**, 112–117. (doi:10.1016/j.jhevol.2007.07.005)
44 Alexander, R. McN. 1991 Characteristics and advantages of human bipedalism. In *Biomechanics in evolution* (eds J. M. V. Rayner & R. J. Wooton), pp. 255–266. Cambridge, UK: Cambridge University Press.
45 Crompton, R. H., Li, Y., Wang, W., Günther, M. & Savage, R. 1998 The mechanical effectiveness of erect and 'bent-hip, bent-knee' bipedal walking in *Australopithecus afarensis*. *J. Hum. Evol.* **35**, 55–74. (doi:10.1006/jhev.1998.0222)
46 Elftman, H. & Manter, J. 1935 Chimpanzee and human feet in bipedal walking. *Am. J. Phys. Anthropol.* **20**, 69–79. (doi:10.1002/ajpa.1330200109)
47 DeSilva, J. M. 2010 Revisiting the 'midtarsal break'. *Am. J. Phys. Anthropol* **141**, 245–258. (doi:10.1002/ajpa.21140)
48 Wunderlich, R. E. 1999 *Pedal form and plantar pressure distribution in anthropoid primates*. PhD thesis, Bell & Howell UMI Dissertation Services, Ann Arbor, USA.
49 Vereecke, E. E., D'Août, K., De Clercq, D., Van Elsacker, L. & Aerts, P. 2005 Functional analysis of the gibbon foot during terrestrial bipedal walking: plantar pressure distributions and 3D ground reaction forces. *Am. J. Phys. Anthropol.* **128**, 659–669. (doi:10.1002/ajpa.20158)
50 Lundgren, P., Nester, C., Liu, A., Arndt, A., Jones, R., Stacoff, A., Wolf, P. & Lundberg, A. 2008 Invasive in vivo measurement of rear-, mid- and forefoot motion during walking. *Gait Posture* **28**, 93–100. (doi:10.1016/j.gaitpost.2007.10.009)
51 Ward, C. V., Kimbel, W. H. & Johanson, D. C. 2011 Complete fourth metatarsal and arches in the foot of *Australopithecus afarensis*. *Science* **331**, 750–753. (doi:10.1126/science.1201463)
52 D'Août, K., Aerts, P., De Clercq, D., De Meester, K. & Van Elsacker, L. 2002 Segment and joint angles of hind limb during bipedal and quadrupedal walking of the bonobo (*Pan paniscus*). *Am J. Phys. Anthropol.* **119**, 37–51. (doi:10.1002/ajpa.10112)
53 Gebo, D. L. & Schwartz, G. T. 2006 Foot bones from Omo: implications for hominid evolution. *Am. J. Phys. Anthropol.* **129**, 499–511. (doi:10.1002/ajpa.20320)
54 Ker, R. F., Bennett, M. B., Bibby, S. R., Kester, R. C. & Alexander, R. McN. 1987 The spring in the arch of the human foot. *Nature* **325**, 147–149. (doi:10.1038/325147a0)
55 Sarmiento, E. 1991 Functional and phylogenetic implications of the differences in the pedal skeleton of australopithecines. *Am. J. Phys. Anthropol.* **12**(suppl.), 157.
56 Berillon, G. 2003 Assessing the longitudinal structure of the early hominid foot: a two-dimensional architecture analysis. *Hum. Evol.* **118**, 113–122. (doi:10.1007/BF02436280)
57 DeSilva, J. M. & Throckmorton, Z. J. 2010 Lucy's flat feet: the relationship between the ankle and rearfoot arching in early Hominins. *PLoS ONE* **5**, e14432. (doi:10.1371/journal.pone.0014432)
58 Tuttle, R. H. 1987 Kinesiological inferences and evolutionary implications from Laetoli bipedal trails G-1, G-2/3 and A′. In *Laetoli: a Pliocene site in Northern Tanzania* (eds M. D. Leakey & J. M. Harris), pp. 503–523. Oxford, UK: Oxford University Press.
59 Proctor, D. J. 2010 Shape analysis of the MT 1 proximal articular surface in fossil Hominins and shod and unshod *Homo*. *Am. J. Phys. Anthropol.* **143**, 631–637. (doi:10.1002/ajpa.21404)
60 Carrier, D. R., Heglund, N. C. & Earls, K. D. 1994 Variable gearing during locomotion in the human musculoskeletal

system. *Science* **265**, 651–653. (doi:10.1126/science.8036513)

61 Li, Y., Crompton, R. H., Günther, M. M., Alexander, R. McN. & Wang, W. J. 1996 Characteristics of ground reaction forces in normal and chimpanzee-like bipedal walking by humans. *Folia Primatol.* **66**, 13–159. (doi:10.1159/000157191)

62 MacConaill, M. A. 1954 The postural mechanism of the human foot. *Proc. R. Irish Acad.* **50B**, 265–278.

63 Caravaggi, P., Pataky, T., Goulermas, J. Y., Savage, R. & Crompton, R. H. 2009 A dynamic model of the windlass mechanism of the foot: evidence for early stance phase preloading of the plantar aponeurosis. *J. Exp. Biol.* **212**, 2491–2499. (doi:10.1242/jeb.025767)

64 Hicks, J. H. 1953 The mechanics of the foot. II. The plantar aponeurosis and the arch. *J. Anat.* **88**, 25–30.

65 Latimer, B., Lovejoy, C. O., Johansen, D. C. & Coppens, Y. 1982 Hominid tarsal, metatarsal, and phalangeal bones recovered from the Hadar formation: 1974–1977 collections. *Am. J. Phys. Anthropol.* **57**, 701–719. (doi:10.1002/ajpa.1330570412)

66 Susman, R. L. & Brain, T. M. 1988 New first metatarsal from Swartkrans and the gait of *Paranthropus robustus*. *Am. J. Phys. Anthropol.* **77**, 7–15. (doi:10.1002/ajpa.1330770103)